

Homolytic aromatic radical perfluoroalkyl-group substitution of arenes in water

Al Postigo*

Departamento de Química Orgánica, Facultad de Farmacia y Bioquímica, Universidad de Buenos Aires. Junín 954 CP 1113, Buenos Aires, Argentina

ABSTRACT

The substitution reaction of aromatic nuclei, such as *N,N*-dialkylated aromatic amines and methoxy-substituted arenes with perfluoroalkyl R_f groups was accomplished *in water* by a photoinduced method to yield the substitution products resulting from replacement of aromatic H's with the R_f moiety in good yields (57-88%). Mechanistic aspects are discussed giving support for a photoinduced electron transfer substitution (PET) reaction. A radical chain mechanism superimposed with a redox process is proposed to account for product formation, as evidenced by the observation of the UV-*vis* transient spectra of the radical cation species generated from electron-rich aromatic compounds in the presence of perfluoroalkyl halides by Nanosecond Laser Flash Photolysis (NLFP) techniques.

KEYWORDS: photoinduced electron transfer substitution, radical aromatic substitution in water, organic radical reactions in heterogeneous media, perfluoroalkyl radicals in water, perfluoroalkylation substitution of aromatic nuclei, radical cations

1. INTRODUCTION

As opposed to radical perfluoroalkylation addition reactions of unsaturated compounds, [1, 2a] fluoroalkyl radical substitution on the aromatic ring has received scarce attention. Furthermore, aromatic

radical perfluoroalkylation in aqueous mixtures is restricted to few examples of sulfinate dehalogenation reactions [2b].

Radical perfluoroalkylation reactions involving arenes in aqueous media have also been reviewed [3]. In particular, activated aromatic nuclei, such as 1,3,5-trimethoxybenzene were employed in perfluoroalkyl substitution radical reactions. When a mixture of 1,3,5-trimethoxybenzene and 1,2-dibromo-1,1,2,2-tetrafluoroethane is treated under sulfinate dehalogenation reaction conditions ($\text{Na}_2\text{S}_2\text{O}_4/\text{NaHCO}_3$ in MeCN/ H_2O), a radical substitution reaction of H for R_f is achieved, according to Scheme 1, [4].

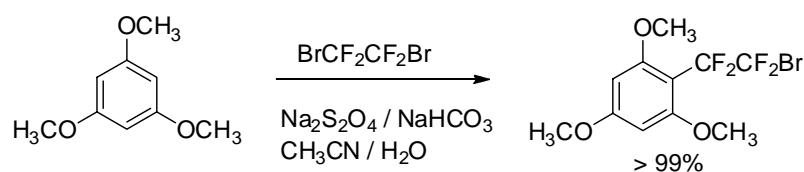
The authors [4] postulate a radical mechanism such as that depicted in Scheme 2.

In another report by the same leading author [5], the aromatic substitution of pyrroles with $\text{BrCF}_2\text{CF}_2\text{Br}$ in aqueous media was achieved rendering the 2-substituted pyrroles in *ca.* 85% yield.

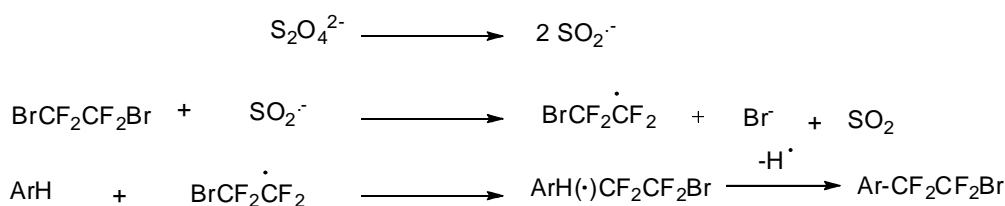
More recently, Lü and collaborators [6] have accomplished the polyfluoroalkylation of 2-aminothiazoles and derivatives, according to Scheme 3. Reactions of 2-aminothiazole with *n*- $\text{C}_4\text{F}_9\text{I}$ under sulfinate dehalogenation reaction conditions, afford the substitution product in 80% yield with total selectivity at the 5-position of 2-aminothiazole (Scheme 3). A number of *N*-substituted 2-aminothiazoles also reacts with $R_f\text{-I}$ and $R_f\text{-Br}$ in yields ranging from 58 to 90%, [6].

While de-fluorination of polyfluoroalkyl-substituted arenes followed by nucleophilic attack from water has been well documented [7], very few reductive

*apostigo@ffyb.uba.ar

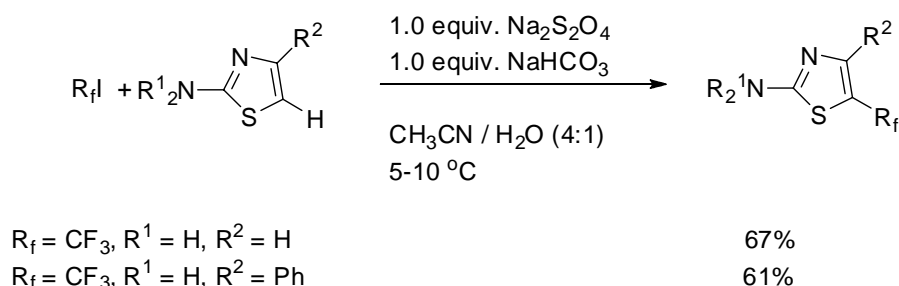


Scheme 1. Synthesis of R_f -substituted arenes by sulfinatodehalogenation reaction.



ArH = 1,3,5-trimethoxybenzene

Scheme 2. Mechanism for the aromatic radical substitution reaction of H for R_f groups.



Scheme 3. Radical perfluoroalkylation of 2-aminothiazole derivatives.

defluorinations of polyfluoroalkyl-substituted arenes under mild conditions have been previously reported, and no other such reaction documented in aqueous media.

Chen and collaborators [8] achieved the radical perfluoroalkylation reaction of aromatic amines by substitution of aromatic H's for R_f groups in DMSO as solvent, triggered through the decomposition of $\text{Na}_2\text{S}_2\text{O}_4$. They attained a series of 2-substituted 1,4-diaminobenzenes with R_f moieties, which upon further reaction afforded intramolecular cyclization products [9].

More recently, Yamakawa and collaborators have accomplished the fluorination of aromatic compounds using the Fenton reagent in DMSO as solvent, in a metal-induced electron transfer-like

reaction [10a, 10b]. They attempted a series of simple-substituted aromatic and heteroaromatic compounds with CF_3I and ethoxycarbonyl difluoromethyl bromide as fluorinating agents.

A photochemical method was successfully employed to effect perfluoroalkylation reactions of aromatic and heteroaromatic compounds to provide substitutions with the corresponding α -aryl- α,α -difluoroacetates and α -aryl- α,α -difluoromethylphosphonates in good to moderate yields [10c]. Photonucleophilic aromatic substitution of 6-fluoroquinolones has also been successfully accomplished in water [11a].

As far as we are concerned, the metal-free photoinduced electron transfer (PET) methodology has not been employed in water or aqueous mixtures

to accomplish the perfluoroalkyl substitution reaction of aromatic nuclei efficiently.

In this account, we will demonstrate that for electron-rich nuclei such as *N,N*-dialkyl-substituted aromatic amines, and methoxy-substituted aromatics, PET *does* take place in water in the presence of perfluoroalkyl iodides (and bromides), rendering this methodology appropriate for the synthesis of fluorinated aromatics in the heterogeneous water environment. Evidence for a radical chain-ion process and singlet-excited state reactivity will be provided.

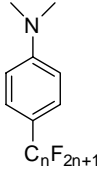
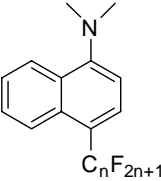
2. MATERIALS AND METHODS

General methods

The internal standard method was used for quantitative GC analysis using authentic samples, and one of the following capillary columns was employed (1% Phenyl-SiO phase): 5 m X 0.53 mm i.d. or 30 m X 0.32 mm i.d. Oven program: starting at 50°C for 5 min, followed by an increase of 5°C/min up to 250°C. NMR spectra were recorded at 400 MHz (for ^1H) or 100.6 MHz (for ^{13}C) or 376.17 MHz (for ^{19}F) in CDCl_3 as deuterated solvent and referenced with the residual solvent peak at 7.26 ppm in the ^1H NMR spectra, 77.0 ppm (CDCl_3) in the ^{13}C NMR spectra, and an external CF_3COOH reference for ^{19}F NMR spectra, respectively. Hydrogen multiplicity (CH , CH_2 , CH_3) information was obtained from carbon DEPT-135 experiments. Some NMR spectral data connectivity was confirmed by ^1H - ^{13}C HSQC and HMBC 2-D experiments. Mass spectra were acquired through direct insertion in a probe heated at 180°C, monitoring the ion current. FT-IR spectra were obtained with 4 cm^{-1} resolution of sample-impregnated NaBr pellets. UV-vis, fluorescence and NLFP experiments were carried out in conventional instruments. Reduced pressure distillation employed a bulb-to-bulb distillation apparatus with four glass bulbs. When necessary, compounds were isolated by flash chromatography performed on silica gel. High-resolution mass spectrometry measurements were performed with a resolution of 1-5 ppm.

Water was obtained from a milli-pore system, and extraction and chromatographic solvents were HPLC-grade. Products from Table 1, and

Table 1. Photoinduced (365 nm-irradiation, 4 h) Substitution of **1** (5 mmol) and **2** (5 mmol) with $\text{C}_n\text{F}_{2n+1}\text{X}$ (1 mmol) in Ar-de-oxygenated water.

R_fX	Product (yield, %)	
$\text{C}_n\text{F}_{2n+1}\text{X}$		
$n = 4, \text{X} = \text{I}$	3 (88)	4 (57)
$n = 8, \text{X} = \text{I}$	5 (86)	6 (68)
$n = 8, \text{X} = \text{Br}$	5 (82)	6 (62)

section 3.1.- were characterized by standard spectroscopic techniques and compared with spectral data from the literature when available.

Materials

Perfluoroalkyl iodides and bromides were commercially available and used as received from the supplier. Aromatic substrates were also commercially available and were previously distilled and stored over molecular sieves (4 Å) prior to use.

Methods of irradiation

Irradiations were conducted with an unfiltered medium pressure Hg lamp ($\lambda_{\text{max}} = 365 - 366 \text{ nm}$) in water-cooled 20 mL or 30 mL Pyrex vessels. The temperature was maintained constantly at 20°C by means of a circulating coolant liquid in the internal vessel. The assembly was maintained at 20 cm from the lamp. The water-heterogeneous mixtures of substrates (5 mmol) and R_fX (1 mmol) were previously deoxygenated by means of a continuous stream of Ar for 15 minutes prior to irradiation. The vessels contained a stirring bar and the mixtures were stirred continuously by means of a magnetic stirrer placed underneath the vessel during the whole irradiation (4 h). After photolysis, the heterogeneous mixtures were extracted into CH_2Cl_2 thrice and the organic layers gathered and dried through an anhydrous Na_2SO_4 -packed column. The extracts were concentrated under reduced pressure, and column-chromatographed through a silica-gel with CH_2Cl_2 : heptane 50:50 or vacuum distilled. Irradiations at

254 nm (three 254 nm-20 watts lamps) were conducted in 15 mL-quartz cells with under vigorous stirring. The vessels were placed at 4 cm of the lamps. Irradiations with fluorescent 350 nm Hg lamps (2 x 40 watts) were conducted with commercial two Actinic BL 40 w –lamps (BaSi₂O₅, Pb phosphor) in a 30-mL vessel in deoxygenated water with constant stirring during 4 h at 2 cm distance from the lamps.

Actinometry

The actinometry was carried out at 365 nm (unfiltered medium pressure Hg lamp). The conversion of the actinometer (potassium ferrioxalate) was monitored by measuring the absorbance of the complex Fe–(*o*-phenanthroline) at 510 nm. A radiant power of ca. 4×10^{-9} einsteins s⁻¹ was achieved after 20 min irradiation. The conversion of **2** was followed by gas chromatographic techniques and kept as low as 5%. Product and substrate concentrations were determined relative to an internal standard (eicosane) and were corrected for relative FID response. The global mass balance exceeded 95%. All were run in duplicate parallel experiments and averaged over two determinations each (see Table 4). The sample and the actinometer (duplicates) were placed equidistant to the lamp in a fixed arrangement. The preparation of the actinometer, potassium ferrioxalate, K₃Fe(C₂O₄)₃ x 3H₂O, was according to the protocol suggested by Hatchard and Parker.

Spectroscopic characterization of known compounds

(*N,N*-Dimethyl-4-(1,1,2,2,3,3,4,4,4-nonafluorobutyl) Benzeneamine) (**3**): 88%, 56 mg (starting from **1** (1 mmol), *n*-C₄F₉I (0.2 mmol)). ¹H NMR δ_H ppm (300.01 MHz, CDCl₃) 3.02 (s, 6H, Me), 6.76 (d, 2H, *J* = 8.80 Hz), 7.41 (d, 2H, *J* = 8.80 Hz). ¹³C NMR δ_C ppm (100.6 MHz, CDCl₃) 40.4 (Me), 111.5 (CH), 128.3 (CH), 152.8 (C). ¹⁹F NMR δ_F ppm (376.17 MHz, CDCl₃) -81.48 (CF₃), -109.84 (CF₂), -123.27 (CF₂), -126.04 (CF₂). GC/MS EI, *m/z* (%). 339 (M⁺, 50), 320 (10), 170 (100). FT-IR (ν, cm⁻¹). 1618 (s), 1350 (m), 1234 (broad s), 1201 (broad s), 868 (m), 810 (m), 741 (m).

(*N,N*-Dimethyl-4-(1,1,2,2,3,3,4,4,5,5,6,6,7,7,8,8,8-heptafluorooctyl) benzeneamine) (**5**): 86%, 463 mg. ¹H NMR δ_H ppm (300.01, CDCl₃) 3.02

(s, 6H, Me), 6.73 (d, 2H, *J* = 8.80 Hz), 7.40 (d, 2H, *J* = 8.80 Hz). ¹³C NMR δ_C ppm (100.6 MHz, CDCl₃) 40.1 (Me), 111.3 (CH), 127.9 (CH), 152.3 (C). ¹⁹F NMR δ_F ppm (376.17 MHz, CDCl₃) -81.29 (CF₃), -109.70 (CF₂), -120.56 (CF₂), -121.71 (CF₂), -122.12 (CF₂), -122.40 (CF₂), -123.18 (CF₂), -126.61 (CF₂). GC/MS EI, *m/z* (%). 539 (M⁺, 15), 520 (5), 170 (100). FT-IR (ν, cm⁻¹). 1618 (s), 1533 (m), 1368 (m), 1242 (br s), 1151 (br s), 815 (m), 655 (m).

(1-Methoxy-4-(1,1,2,2,3,3,4,4,4-nonafluorobutyl) benzene) (**10a**) yellowish oil, 85%, 11 mg. ¹H NMR δ_H ppm (300.01 MHz, CDCl₃) 3.85 (s, 3H, Me), 7.01 (d, *J* = 7.7 Hz, 2H), 7.50 (d, *J* = 8.1 Hz, 2H). ¹³C NMR δ_C ppm (100.6 MHz, CDCl₃) 55.3, 120.3, 120.8, 133.6, 159.7. ¹⁹F NMR δ_F ppm (376.17 MHz, CDCl₃) -81.09, -110.34, -122.38, -125.82. FT-IR (ν, cm⁻¹). 2923 (s), 1583 (m), 1336 (m), 1203 (m), 992 (m).

(1-Methoxy-2-(1,1,2,2,3,3,4,4,4-nonafluorobutyl) benzene) (**10b**) yellowish oil, 85%, 9 mg. ¹H NMR δ_H ppm (300.01 MHz, CDCl₃) 3.85 (s, 3H, Me), 7.01 (m, 1H), 7.12 (m, 1H), 7.50 (m, 2H). ¹³C NMR δ_C ppm (100.6 MHz, CDCl₃) 55.8, 112.4, 117.6, 128.4, 128.5, 129.2, 158.5. ¹⁹F NMR δ_F ppm (376.17 MHz, CDCl₃) -81.21, -110.75, -122.98, -125.96.

Spectroscopic characterization of unknown compounds

(*N,N*-Dimethyl-4-(1,1,2,2,3,3,4,4,4-nonafluorobutyl) naphthalene-1-amine) (**4**): yellowish oil, yield 86 mg (57%). ¹H NMR (400.1 MHz, CDCl₃) δ_H ppm 2.95 (s, 6H, Me), 7.05 (d, 1H, *J* = 8.1 Hz), 7.41 (t, 1H, *J* = 8.06 Hz, 7.97 Hz), 7.54 (m, 3H), 7.70 (d, 1H, *J* = 8.25 Hz). ¹³C NMR (100.6 MHz, CDCl₃) δ_C ppm 45.2 (Me), 112.4 (C), 118.3 (CH), 123.3 (CH), 124.5 (CH), 125.6 (CH), 126.1 (CH), 129.2 (C), 132.2 (C), 155.6 (C). ¹⁹F NMR (376.17 MHz, CDCl₃) δ_F ppm -81.32 (CF₃), -111.64 (CF₂), -123.3 (CF₂), -126.17 (CF₂). FT-IR (ν, cm⁻¹). 2945 (m), 1581 (s), 1234 (broad, s), 1098 (broad, s), 806 (broad, s). GC/MS EI, *m/z* (%). 389 (M⁺, 95), 370 (18), 220 (100). ESI-HRMS Anal. Calcd for C₁₆H₁₂F₉N 389.0826, found 389.0876. Elemental analyses: Found: C (49.05%), H (3.71%), N (3.21%). Calcd for C₁₆H₁₂F₉N: C (49.37%), H (3.11%), F (43.93%), N (3.60%).

(*N,N*-Dimethyl-4-(1,1,2,2,3,3,4,4,5,5,6,6,7,7,8,8,8-heptafluorooctyl)-naphthalene-1-amine) (**6**): yellowish oil, yield 68% (25 mg). ^1H NMR (400.1 MHz, CDCl_3) δ_{H} ppm 2.96 (s, 6H, Me), 7.08 (d, 2H, $J = 8.06$ Hz), 7.54 (m, 2H), 7.71 (m, 1H, $J = 8.25$ Hz), 8.18 (d, 1H, $J = 7.52$ Hz). ^{13}C NMR (100.6 MHz, CDCl_3) δ_{C} ppm 45.1 (Me), 115.7 (C), 124.9 (CH), 125.6 (CH), 127.4 (CH), 128.3 (CH), 128.4 (CH), 131.7 (C). ^{19}F NMR (376.17 MHz, CDCl_3) δ_{F} ppm -81.16 (CF_3), -107.47 (CF_2), -120.53 (CF_2), -121.70 (CF_2), -122.12 (CF_2), -122.30 (CF_2), -123.09 (CF_2), -126.49 (CF_2). FT-IR (ν , cm^{-1}). 2962 (m), 1582 (m), 1242 (broad, s), 1210 (broad, s), 802 (broad, s). GC/MS EI, m/z (%). 589 (7), 220 (100). ESI-HRMS Anal. Calcd for $\text{C}_{20}\text{H}_{12}\text{F}_{17}\text{N}$ 589.0698, found 589.0658. Elemental analyses: Found: C (40.05%), H (2.61%), N (2.41%). Calcd for $\text{C}_{20}\text{H}_{12}\text{F}_{17}\text{N}$: C (40.76%), H (2.05%), F (54.81%), N (2.38%).

(*N*-Methyl-4(1,1,2,2,3,3,4,4,4-nonafluorobutyl) benzeneamine) (**9**): yellowish oil, yield 45 mg (32%). ^1H NMR (400.1 MHz, CDCl_3) δ_{H} ppm 2.98 (s, 3H, Me), 6.77(d, 2H, $J = 9$ Hz), 7.48 (m, 2H). ^{13}C NMR (100.6 MHz, CDCl_3) δ_{C} ppm 30.7, 118.4, 125.6, 149.6. ^{19}F NMR (376.17 MHz, CDCl_3) δ_{F} ppm -80.32 (CF_3), -110.48 (CF_2), -123.45 (CF_2), -125.54 (CF_2). FT-IR (ν , cm^{-1}). 3348 (w), 2964 (m), 1261 (s), 1093 (broad, s), 1027 (broad, s), 800 (s). GC/MS EI, m/z (%) 325 (1), 310 (17), 220 (100). EI-HRMS Anal. Calcd for $\text{C}_{11}\text{H}_8\text{F}_9\text{N}$ 325.0513, found 325.0514. Elemental analyses: Found: C (40.05%), H (2.71%), N (4.21%). Calcd for $\text{C}_{16}\text{H}_{12}\text{F}_9\text{N}$: C (40.63%), H (2.48%), F (52.58%), N (4.31%).

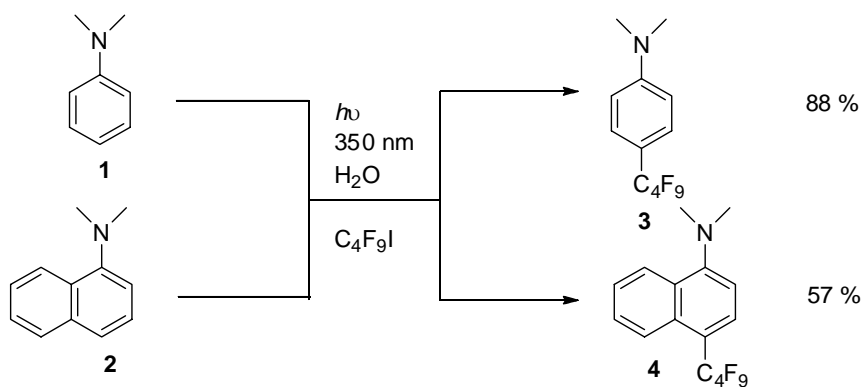
(*N*-Methyl-4(1,1,2,2,3,3,4,4,4-nonafluorobutyl) benzeneamine) (**11**): yellowish oil, yield 45 mg (32%). ^1H NMR (400.1 MHz, CDCl_3) δ_{H} ppm 2.98 (s, 3H, Me), 6.77(d, 2H, $J = 9$ Hz), 7.48 (m, 2H). ^{13}C NMR (100.6 MHz, CDCl_3) δ_{C} ppm 30.7, 118.4, 125.6, 149.6. ^{19}F NMR (376.17 MHz, CDCl_3) δ_{F} ppm -80.32 (CF_3), -110.48 (CF_2), -123.45 (CF_2), -125.54 (CF_2). FT-IR (ν , cm^{-1}). 3348 (w), 2964 (m), 1261 (s), 1093 (broad, s), 1027 (broad, s), 800 (s). GC/MS EI, m/z (%) 325 (1), 310 (17), 220 (100). EI-HRMS Anal. Calcd for $\text{C}_{11}\text{H}_8\text{F}_9\text{N}$ 325.0513, found 325.0514. Elemental analyses: Found: C (40.05%), H (2.71%), N (4.21%). Calcd for $\text{C}_{16}\text{H}_{12}\text{F}_9\text{N}$: C (40.63%), H (2.48%), F (52.58%), N (4.31%).

3. RESULTS AND DISCUSSION

3.1. Aromatic substitution reactions of *N,N*-dimethylaniline and *N,N*-dimethyl-1-naphthyl amine with R_fX in water

When we subject an Ar-deoxygenated heterogeneous mixture of *N,N*-dimethylaniline **1** or *N,N*-dimethyl-1-naphthyl amine **2** [11b, 11c] and *n*- $\text{C}_4\text{F}_9\text{I}$ in water under vigorous stirring to the photoinduced reaction (medium pressure Hg lamp, $\lambda_{\text{max}} = 365$ nm), we obtain the nonafluorobutyl *para* substitution product **3** and the *4*-position substitution product **4**, respectively, in yields ranging from 57 to 88%, based on *n*- $\text{C}_4\text{F}_9\text{I}$, according to Scheme 4, Table 1.

The product yields increase upon increasing the concentration of substrates. Thus the best product yields are obtained when the *substrate:n-C₄F₉I* ratio is *ca.* 5:1.



Scheme 4. Perfluorobutyl group substitution of aromatic amines in water.

The UV-visible spectra of substrates **1**, **2** and reagent $n\text{-C}_4\text{F}_9\text{I}$ are depicted in Figure 1.

When reaction conditions are changed to 254 nm-irradiation and increasing the $n\text{-C}_4\text{F}_9\text{I}$:substrate ratio to 5:1 instead, substitution of the aromatic moiety with the R_f group is also achieved with similar efficiency.

Under our reaction conditions, and given the optical density at 254 nm of mixtures of **1** or **2** with $n\text{-C}_4\text{F}_9\text{I}$, appreciable homolysis of C-I bond from $n\text{-C}_4\text{F}_9\text{-I}$ is expected. The presence of substitution products under these reaction conditions (254 nm-irradiation) might indicate that direct homolysis of $n\text{-C}_4\text{F}_9\text{I}$ could be involved in the substitution mechanism as a rate limiting step.

In order to cast some light into the reactive excited state manifold of substrate **1** (or **2**), we carried out product studies of the PET reaction (at irradiation wavelength $\lambda = 310$ nm) of **1** (one equivalent), in the presence of $n\text{-C}_4\text{F}_9\text{I}$ (one equivalent) and 4-methoxyacetophenone (15 equivalents), a good known triplet energy sensitizer ($E_T = 310$ KJ mol⁻¹). Under these reaction conditions, no substitution product **3** (or **4** from substrate **2**) was encountered (*i.e.*: $E_{T(2)} = 226$ KJ mol⁻¹ [11c]). This would seem to imply that the singlet excited state manifold is responsible for the aromatic substitution product in water, and that sensitized population of the triplet state of the

amine does not lead to an aromatic substitution reaction [11b, d].

The $n\text{-C}_4\text{F}_9\bullet$ radical shows a clear-cut electrophilic character in the aromatic substitution, as already reported for the addition to alkenes [12, 13], but the low regio- and chemoselectivity suggest that the polar effect is not the main factor in determining the high reactivity of perfluoroalkyl radicals toward aromatics ($10^5\text{-}10^6$ dm³mol⁻¹ s⁻¹, 2-3 orders of magnitude more reactive than alkyl radicals). The enthalpic factor, related to the involved bond energies, appears to be the major cause of the increased reactivity. The polar effect is considered as related more to the polarizability than to the polarity of a radical (the σ -perfluoroalkyl radicals are considered less polarizable and hence less sensitive to polar effects than σ -carbon radicals) [14].

We also subjected substrates **1** and **2** to the photoinduced (365 nm) substitution reaction with $\text{C}_n\text{F}_{2n+1}\text{X}$ ($n = 6, 8$; $\text{X} = \text{I}, \text{Br}$) in water, obtaining substitution products in yields indicated in Table 1.

In a typical radical addition reaction of $\text{R}_f\bullet$ radicals derived from $\text{C}_n\text{F}_{2n+1}\text{X}$ ($n = 4, 6, 8, 10$, $\text{X} = \text{I}, \text{Br}$) onto different alkenes under various radical initiation methodologies in water, the lower yields of addition products derived from $\text{R}_f\text{-Br}$ have been interpreted as resulting from a higher BDE of $\text{R}_f\text{-Br}$ as compared to $\text{R}_f\text{-I}$ in the radical addition mechanism [1].

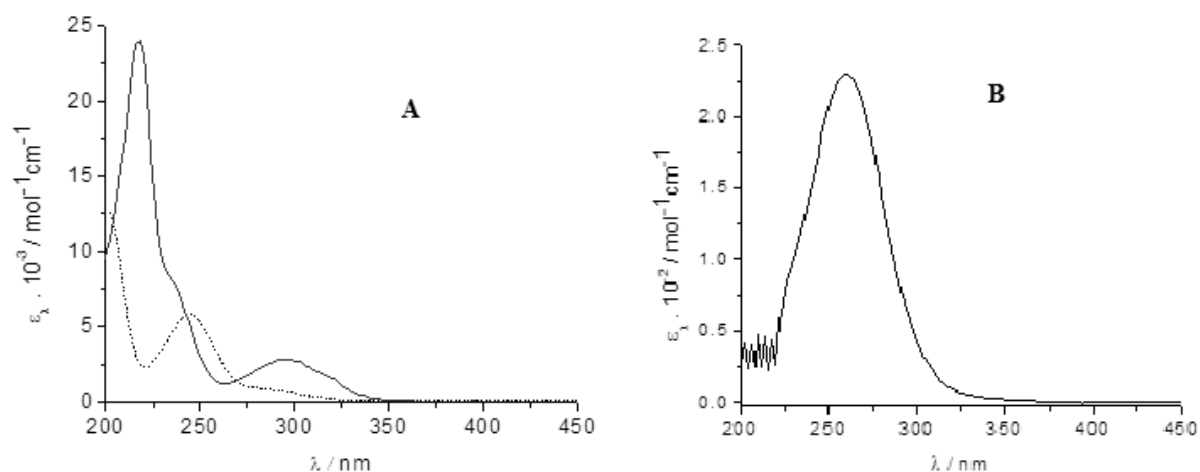


Figure 1. A: UV-visible spectra of substrates **1** (···) and **2** (—) in H₂O, λ_{max} (**1**) = 242 nm ($\epsilon = 5705$ dm³ mol⁻¹cm⁻¹), 287 nm ($\epsilon = 1145$ dm³ mol⁻¹cm⁻¹); λ_{max} (**2**) = 218 nm ($\epsilon = 2.4 \times 10^5$ dm³ mol⁻¹cm⁻¹), 294 nm ($\epsilon = 2741$ dm³ mol⁻¹cm⁻¹). **B:** UV-visible spectrum of $n\text{-C}_4\text{F}_9\text{I}$ in MeCN, $\lambda_{\text{max}} = 262$ nm (2300 dm³ mol⁻¹cm⁻¹).

We undertook a kinetics study on product **6** formation when **2** reacts with either *n*-C₈F₁₇I or with *n*-C₈F₁₇Br in water under 365 nm-irradiation under the same conditions depicted in Table 1, and observed a steady increase in the yields of **6** (arising from either *n*-C₈F₁₇I or from *n*-C₈F₁₇Br) independently of the perfluoroalkyl halide utilized (Figure 2, Table 2). This would seem to imply that R_f – X bond homolysis is not a rate-limiting step in the photo-substitution mechanism.

We also undertook the PET reaction (365 nm-irradiation) of **2** (5 mmol) in the presence of *n*-C₄F₉I (1 mmol) in MeCN (30 mL) as solvent, and obtained the substitution product **4**, albeit in lower yields (46%).

3.2. Intermolecular interactions in the ground and excited states and PET mechanism

We could not find a charge transfer complex (CTC) in the UV-*vis* spectra of **1** or **2** upon addition

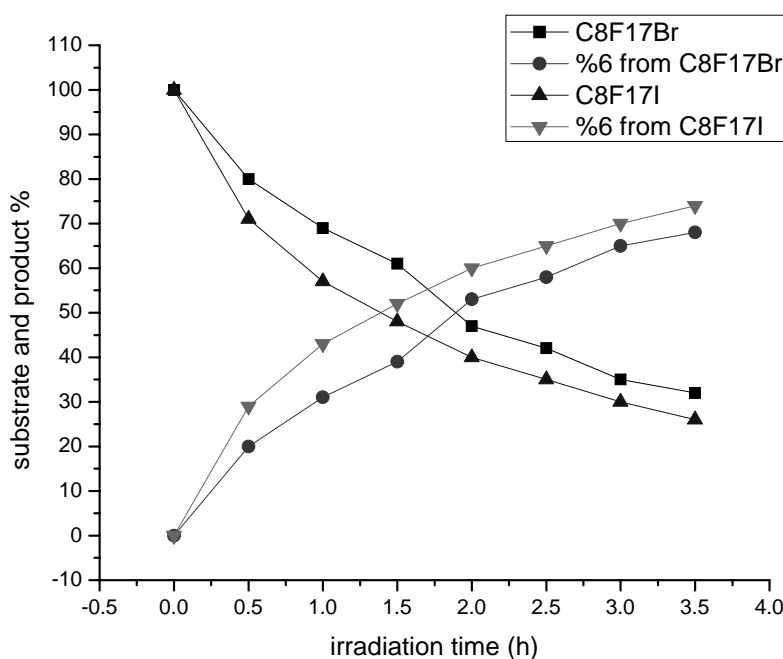


Figure 2. Plots of % substrates C₈F₁₇Br(■), C₈F₁₇I (Δ)disappearance and product **6** (%) formation from *n*-C₈F₁₇Br (●) and from *n*-C₈F₁₇I (∇) versus irradiation time normalized to 100%

Table 2. Normalized (100%) yields of substrates *n*-C₈F₁₇Br, *n*-C₈F₁₇I disappearance and product **6** (%) formation from *n*-C₈F₁₇Br and *n*-C₈F₁₇I under reaction conditions of Table 1.

Irradiation time	% <i>n</i> -C ₈ F ₁₇ Br	% 6 (from <i>n</i> -C ₈ F ₁₇ Br)	% <i>n</i> -C ₈ F ₁₇ I	% 6 (from <i>n</i> -C ₈ F ₁₇ I)
0	100	0	100	0
0.5	80	20	71	29
1	69	31	57	43
1.5	61	39	48	52
2	47	53	40	60
2.5	42	58	35	65
3	35	65	30	70
3.5	32	68	26	74

of $n\text{-C}_4\text{F}_9\text{I}$ in MeCN as solvent. We performed a series of fluorescence quenching experiments of substrates **1**, **2**, and N -methyl-aniline **7** with $n\text{-C}_4\text{F}_9\text{I}$ in MeCN, in order to obtain Stern-Volmer quenching rate constants K_{sv} in this solvent and henceforth the quenching rate constants of the fluorescence (k_q) of substrates **1**, **2**, and **7** with $n\text{-C}_4\text{F}_9\text{I}$, according to Figure 3 (for substrates **1** and **2**). The values of the singlet lifetimes for

1 and **2** in MeCN:H₂O are 2.24 ns and 2.40 ns, respectively (see Table 3, entry 7).

The quenching of fluorescence of **1** and **2** (and **7**) by $n\text{-C}_4\text{F}_9\text{I}$ supports the PET mechanism. Also, the quenching rate constants (entry 4, Table 3) show a good correlation between the oxidation peak potential of the amine (entry 1, Table 3) and the theoretical values of their HOMO energy calculated by using AM1 method (not shown).

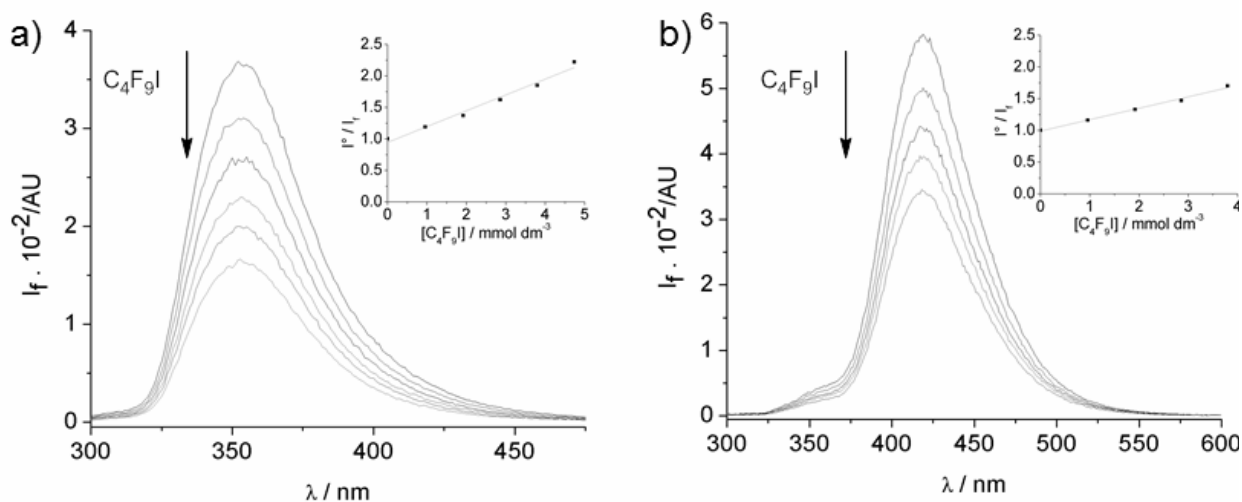


Figure 3. Fluorescence quenching and Stern-Volmer Plots for substrates **1** (a) and **2** (b) with $n\text{-C}_4\text{F}_9\text{I}$ in MeCN.

Table 3. Rehm-Weller parameters for amines **1**, **2**, **7** and $n\text{-C}_4\text{F}_9\text{I}$.

Entry	Compound	Compound			
		1	2	7	$n\text{-C}_4\text{F}_9\text{I}$
1	E_{D/D^+} (V)	+0.71 ^a	+0.39	0.73 ^b	-
2	E_{A/A^-} (V)	-	-	-	-1.27
3	E^* (eV)	3.22 (3.87) ^c	3.39	3.12	
4	Log k_q ($\text{M}^{-1}\text{s}^{-1}$)	8.05	7.88	8.46	
5	ΔG_{ET} (eV)	-1.29	-1.58	-1.78	
6	ΔG_{ET} (Kcal/mol)	-27.3	-36.3	-40.9	
7	τ (ns)	2.24 ^d	2.40 ^e	1.22 ^d	
8	$\phi_{\text{fluorescence}}$	0.042 ^d	0.20 ^f	0.032 ^d	

^aref. [20]. E_{ox} (vs SCE) = 0.83 V.

^bref. [23], measured in water, vs NHE.

^cref. [21]. τ = 2.78 ns

^dref. [22]. τ Measured in water vs NHE.

^eref. [24], measured in CH₂Cl₂

^fref. [17], measured in MeCN:H₂O

We could not find an exciplex formation in the fluorescence of **1** or **2** upon addition of *n*-C₄F₉I, which rules out an emission complex from the ET-couple A (Scheme 5 for **2**).

The fact that substrates' concentrations have to be kept high (2-5 or more equivalents per *n*-C₄F₉I equivalent used) has a two-fold reason: firstly, the optical density of the heterogeneous mixture has to be maintained high enough in substrate in order to minimize or avoid direct photolytic dissociation of *n*-C₄F₉I [15], and secondly, the back ET of the ion-pair A (Scheme 5 for substrate **2**) must be a very efficient process, since at equimolar or lower *substrate*:*R_fI* concentration ratios, lower yields of substitution products are found. In our reaction product mixtures, a mass balance of *ca.* 95% for substrates **1** or **2** and product is encountered, purporting that mostly of the substrates' excess concentration is recovered unaltered.

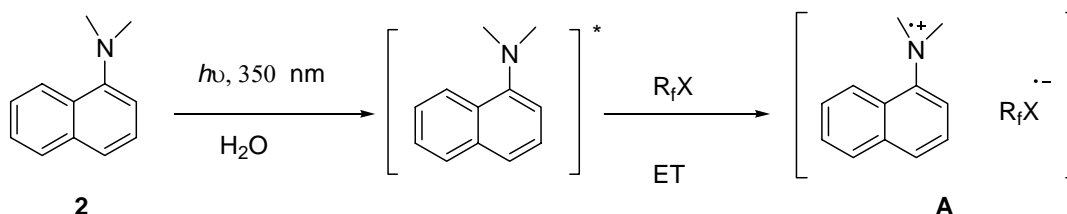
In order to give further support for the ET mechanism in the perfluorobutylation substitution reaction of **1** and **2** in water, we employed the Rehm-Weller equation (eq 1) so as to see whether

the Gibbs energy change in the ET process (ΔG_{ET}) is spontaneous or not.

$$\Delta G^{\circ} = E_{(D/D^{+})} - E_{(A/A^{-})} - E^{*} + \frac{Z_1 Z_2}{\epsilon r_{12}} \quad (1)$$

Where $E_{(D/D^{+})}$ is the redox potential of the donor, and $E_{(A/A^{-})}$ the redox potential of the acceptor, E^{*} the singlet excited state energy of the aromatic amine, and the last term represents the coulombic energy necessary to form an ion pair with charges Z_1 and Z_2 in the medium of dielectric constant ϵ at a distance r_{12} .

From an overlap of the UV-*vis* and fluorescence plots of substrates **1**, **2**, and *N*-methylaniline **7** we calculated the excited state (singlet) energies (E^{*}) for **1**^{*}, **2**^{*}, and **7**^{*}, (Figure 4, for **1**, **2**, and **7**). The redox potential of the donor aromatic amines **1** and **2** are +0.71 V (*versus* SCE, in MeCN) [16] and +0.39 V respectively [17]. The coulombic term was taken as -0.05 eV assuming a separation distance of 0.8 nm [18]. The redox potential of the acceptor *n*-C₄F₉I was taken to be -1.27 V as an approximate measure given in DMF [19].



Scheme 5. PET between **2** and R_fX to generate radical ion Pair A.

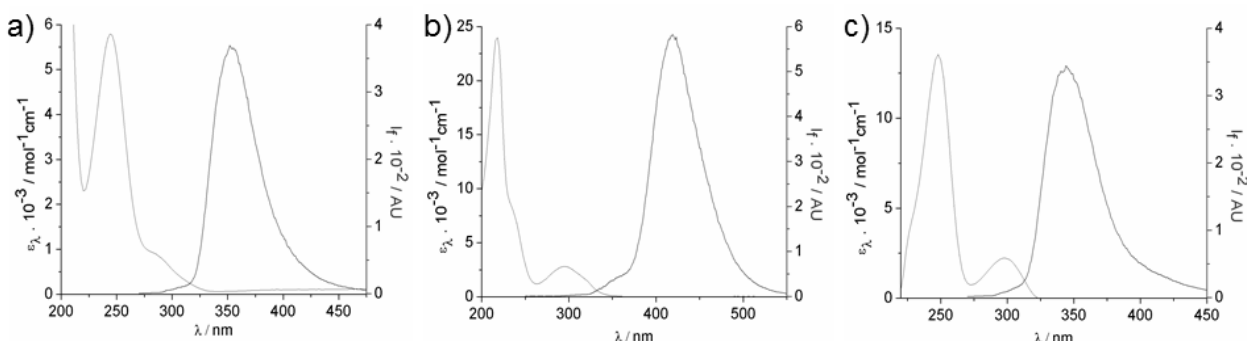


Figure 4. Graphical determination of singlet excited state energies E^{*} from UV-*vis* fluorescence spectra overlaps for substrates **1** (a), **2** (b), and **7** (c) in water.

Thus we calculated ΔG_{ET} from **2** to *n*-C₄F₉I to be -1.58 eV (-36.31 Kcal/mol), and that from **1** to *n*-C₄F₉I to be -1.19 V (-27.34 Kcal/mol), highly spontaneous processes. For comparison, the photoinduced ET addition of **2** to furanone [17] was determined by Hoffmann and collaborators to have a $\Delta G_{\text{ET}} = -0.37$ eV (-8.5 Kcal/mol) in a mixture of MeCN:water. The data are summarized in Table 3 [17]. The remainder of the data for substrate **7** are also collected in Table 3.

Generally speaking, photochemical electron transfer reactions occur only when the charge transfer step is either exergonic or < 5 Kcal/mol [25].

Also in Table 3, measures of $\log k_q$ (logarithm of rate constant for fluorescence quenching of amine substrates with *n*-C₄F₉I) of **1**, **2**, and *N*-methyl aniline **7** are given as a function of ΔG_{ET} , showing that the ET processes are at diffusion rate in MeCN (in water the diffusion rate $8RT/3\eta$ where η is the viscosity of water taken as 8.90×10^{-3} dyn·s/cm² or 0.890 cP at about 25°C). A plot of $\log k_q$ of substrates **1**, **2**, **7** (and substrate 2-methoxynaphthalene, *vide infra*) with *n*-C₄F₉I versus ΔG_{ET} (Figure 5) demonstrates that the ET process has a slope nearing zero, purporting a diffusion-controlled process for these substrates in water.

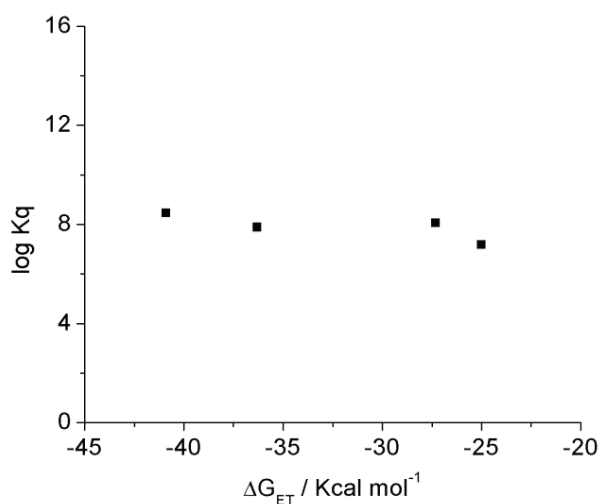


Figure 5. Bimolecular quenching rate constants as a function of the overall gibbs energy change for the Photoinduced Electron-transfer (PET) reaction of **1**, **2**, **7**, and 2-methoxynaphthalene (*vide infra*) with *n*-C₄F₉I in water (Table 3).

It has been established that in the region $\Delta G_{\text{ET}} = -0.5 \sim -2.0$ eV, the primary quenching product is the ground-state geminate radical pairs (GRP, as in **A**, Scheme 5) and it has been confirmed that the rate k_{bet} of back ET within GRP shows a bell-shaped dependence on the free energy change ΔG_{bet} of back ET within geminate radical pairs in agreement with the Marcus theory [26] for long-distance ET [27]. Our obtained ΔG_{ET} values (Table 3, entries 5,6) fall within this full ET region of the ground state radical ion pairs (such as **A** in Scheme 5).

Having established that the triplet excited manifold of **1** or **2** is not responsible for the substitution reaction (*vide supra*), we have to take into account, however, that upon addition of *n*-C₄F₉I, a possible intersystem crossing mechanism could be in operation. If fluorescence quenching is induced by exciplex formation, the triplet yield ϕ_T in fluorescence quenching is expected to be strongly enhanced by a heavy atom substitution on fluorescer and/or quencher, because the intersystem crossing within exciplex can be efficiently enhanced by a heavy atom involved in the fluorescer and/or quencher [28]. If fluorescence quenching is induced by long-distance ET (as is the case when $\Delta G_{\text{fet}} = -0.5 \sim -2.0$ eV), in contrast, ϕ_T is not enhanced by the heavy atom substitution at all, when the energy $E(T_1)$ of lowest excited triplet-state is higher than the energy $|\Delta G_{\text{bet}}|$ of GRP. Even when $E(T_1) < |\Delta G_{\text{bet}}|$, ϕ_T is not so enhanced by the heavy atom substitution, because the spin-orbit interaction within GRP is weak. Therefore, the heavy atom effect on ϕ_T is a measure for determining the quenching mechanism (*vide infra*) [27].

We performed a series of Laser Flash Photolysis (NLFP) experiments of *N,N*-dimethyl-1-naphthylamine **2** in the presence of *n*-C₄F₉I in MeCN as solvent. Figure 6 depicts the transient spectrum of the *N,N*-dimethyl-1-naphthylamine radical cation **2^{•+}** (**B**) in the presence of *n*-C₄F₉I, and that of the triplet-triplet absorption spectrum of **2** in the absence of *n*-C₄F₉I (**A**).

The wavelength maxima in spectrum **B** at 383, 440, and 675 nm, respectively, can be attributed to the radical cation species **2^{•+}** generated after laser pulse excitation (355 nm) of **2** in the presence of

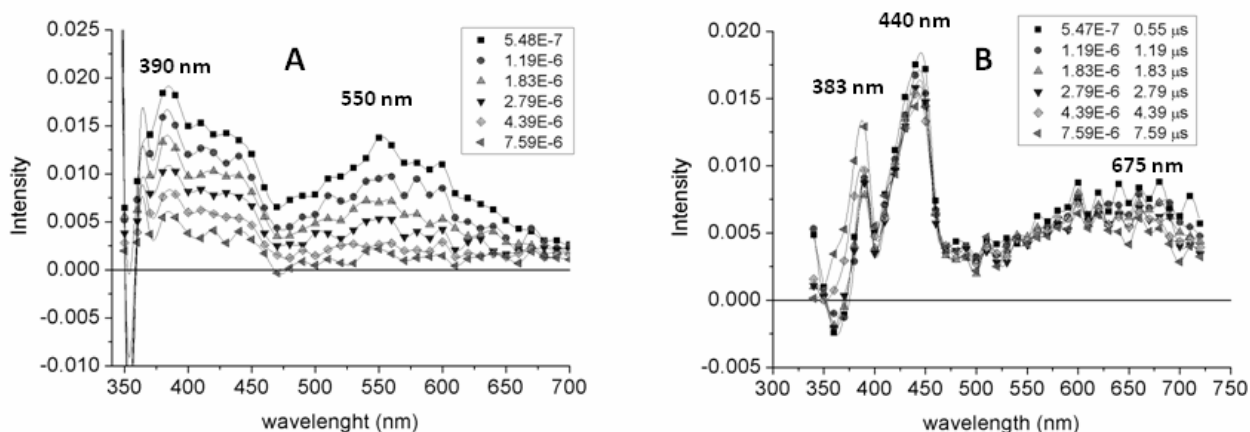


Figure 6. Transient UV-vis spectra of 0.8 mmol dm^{-3} *N,N*-dimethyl-1-naphthylamine **2** in MeCN after 0.55, 1.2, 1.8, 2.8, 4.4, and 7.6 μs of the laser pulsing at 355 nm excitation wavelength: **A**) in the absence of *n*-C₄F₉I. **B**) in the presence of $11.6 \text{ mmol dm}^{-3}$ *n*-C₄F₉I.

n-C₄F₉I, which is in excellent agreement with the reported spectrum of 2^{++} generated after laser pulse excitation of **2** in the presence of benzophenone (radical anion) [11a]. On the other hand, in the absence of *n*-C₄F₉I (spectrum **A**, Figure 6), wavelength maxima at 390 nm and 550 nm can be assigned to the triplet-triplet absorption spectrum of **2** ($^32^*$), also in agreement with reported data [11a]. It is observed from comparison of spectra **A** and **B** in Figure 6, that 2^{++} is a more persistent transient (*i.e.*: longer lived transient) than $^32^*$. This makes the former a better candidate as intermediate in the photosubstitution reaction of amines with R_fI.

The LFP transient experiments show that addition of *n*-C₄F₉I does not provoke enhancement of the spin-orbit coupling in **2** and that the triplet manifold is not a discrete intermediate in the photosubstitution reaction of **2** with R_fI (*cf.* spectrum **A** and **B** in Figure 6).

Shizuka and co-workers [11c,d] showed that in MeCN, triplet energy transfer from triplet benzophenone BP to **2** produces triplet $^32^*$ and the corresponding triplet exciplex, whereas electron transfer took place during the deactivation of triplet BP to yield the benzophenone anion and 2^{++} cation radicals in MeCN-H₂O (4:1 v/v) [11d]. The authors predicted schematically that added water may play an important role in altering the chemical interactions in the BP-**2**. Though we were unable to measure transient spectra in water

or mixtures of water:MeCN of **2** and *n*-C₄F₉I, the claim of the participation of 2^{++} cation radicals in water is reasonable [11c].

We managed to measure the quantum yield of 2^{++} cation radicals production using $^3\text{BP}^*$ in MeCN, and obtained a value of $\phi_{2^{++}} = 0.37$, which is similar, within error, to the quantum yield of fluorescence of **2** (Table 3, entry 8, column 4), purporting that 2^{++} is formed very efficiently within our reaction conditions.

We also managed to measure quantum yields (by ferrioxalate actinometry) of product **4** and **6** formation and substrate **2** disappearance, from photoreaction of **2** with *n*-C₄F₉I and *n*-C₈F₁₇I, respectively, according to Table 4.

It is apparent that substrate **2** shows a quantum efficiency of *ca.* 200, based on substrate consumed, and the quantum yield of also *ca.* 200 for the formation of products **4** and **6**. Clearly, substrate **2** undergoes reaction either with *n*-C₄F₉I or with *n*-C₈F₁₇I by a chain mechanism.

The average values for runs 1 and 2 for substrate **2** consumption quantum yields (upon reaction with *n*-C₄F₉I, entries 1 and 3, Table 4) afford a value of 236 ± 53 , which is, within error, in agreement with an average value for the quantum yield for formation of product **4**, *i.e.*: 221 ± 54 .

Analogously, the average values for runs 1 and 2 for substrate **2** consumption quantum yields (upon reaction with *n*-C₈F₁₇I, entries 2 and 3, Table 4)

Table 4. Quantum yields (ϕ) from the photoreaction (365 nm-irradiation) of **2** (5 mmol) with *n*-C₄F₉I (1 mmol) in Ar de-oxygenated water, to afford product **4**, and those from the photoreaction of **2** (5 mmol) with *n*-C₈F₁₇I (1mmol), to afford product **6** in H₂O^a.

Entry	Run	Substrate/product, (chemical yield, % \pm % ϵ)	Mass balance, %	Substrate/product (quantum yield, $\phi \pm \epsilon$)
1	1	2 ^b (91 \pm 5) / 4 ^c (4 \pm 0.2)	95	2 ^d (241 \pm 48) / 4 ^e (225 \pm 55)
2	1	2 ^b (93 \pm 5) / 6 ^c (5 \pm 0.6)	98	2 ^d (265 \pm 50) / 6 ^e (201 \pm 24)
3	2	2 ^b (92 \pm 5) / 4 ^c (5 \pm 0.3)	97	2 ^d (231 \pm 59) / 4 ^e (217 \pm 54)
4	2	2 ^b (97 \pm 5) / 6 ^c (1 \pm 0.8)	98	2 ^d (254 \pm 47) / 6 ^e (197 \pm 69)

^aConditions: MPL (medium pressure Hg lamp) unfiltered. Irradiation time: 20 min. Determined by ferrioxalate actinometry. All were run in duplicate parallel experiments and averaged over two determinations each.

^b% quantitative yield of substrate recovered, measured by GC

^c% quantitative yield of product formed, measured by GC

^dquantum yield ϕ of substrate disappearance

^equantum yield ϕ of product formed

afford a value of 259 ± 48 , which is, within error, in agreement with an average value for the quantum yield for formation of product **6**, *i.e.*: 199 ± 46 .

Another important mechanistic piece of evidence is provided by the decrease in pH as the photoreaction progresses. The initial pH of the reaction mixture is 5.5. At 2-hour photoreaction, the registered pH is 2.5. This could indicate that proton loss is involved in the reaction mechanism, and that an intermediate such as those postulated in classical aromatic electrophilic substitutions (Wheland intermediate) might be participating in the reaction mechanism.

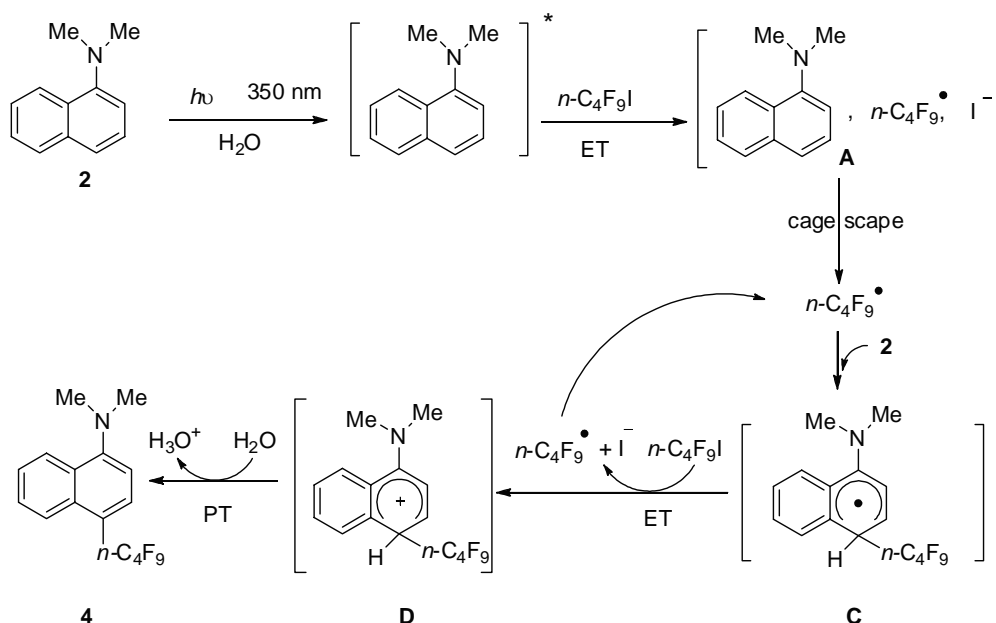
We thus postulate a photoinduced (PET) mechanism, where upon light absorption by substrates **1** or **2**, germinal radical ion pairs (GRP) **A** (in the case of **2**) are formed in the solvent cage (Scheme 6, for substrate **2**). The radical anion *n*-C₄F₉I^{•-} dissociates into *n*-C₄F₉• radicals and iodide anion (Scheme 6). Cage escape of **2**^{•+} (or **1**^{•+}), and *n*-C₄F₉• radicals ensues. The radical *n*-C₄F₉• adds to the 4-position of **2** (and the *para* position of **1**) to render an aromatic substituted radical intermediate **C** (in the case of **2**) which upon ET to *n*-C₄F₉I generates the cation **D** (Wheland intermediate stabilized by resonance effect from the N atom) and regenerates *n*-C₄F₉• radicals (and iodide anion). The very acidic cyclohexadienyl cation species **D** suffers rapid deprotonation in water to render the thermoneutral substitution product **4** and a notable decrease in pH. We expect that

process in step 1 (Scheme 6) to be thermodynamically favorable, since the electron donor ability of **2** should be inherently higher than that of **4**.

It is observed that this is a *chain* PET mechanism, where radicals *n*-C₄F₉• enter the cycle as a radical chain carrier, as summarized in the propagation process depicted in Figure 7.

It is known that pulse radiolysis of *N,N*-dimethylaniline **1** in neutral aqueous solution shows formation of *N*-methylanilinomethyl radicals and radical cations in a 1:2 ratio. The precursor for the two radicals is the OH radical [29]. The radical cation **1**^{•+} is also known to undergo dissociation in the presence of nucleophiles (*i.e.*: H₂O \rightarrow H₃O⁺) to **1**[•] radicals which could further react in the presence of oxygen, such as in eq 2 at diffusion level [30].

Baciocchi and collaborators [31] have also shown that the α -amino carbon radicals such as *N*-methylanilinomethyl radicals shown in eq 2, can be converted to the *N*-demethylated aniline (*i.e.*: *N*-methylaniline **7**), by oxidation of *N*-methylanilinomethyl radicals to a carbinolamine, which in turn is converted to the *N*-methylaniline and CH₂O, which they managed to detect as its dimer adduct [31]. Although in their case the sequence of the oxidation reactions was triggered by the use of phthalimide *N*-oxyl radical (PINO) which generated the radical cation of the



Scheme 6. Postulated PET mechanism for the perfluoroalkylation reaction of arenes in water.

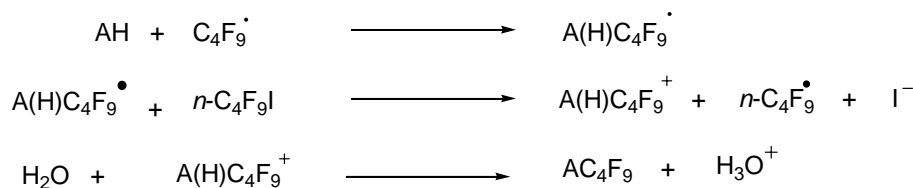
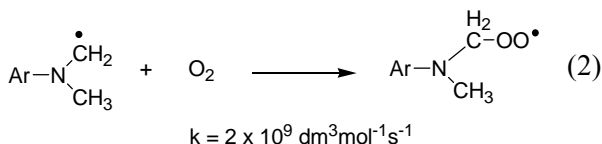


Figure 7. Propagation cycle for the proposed PET chain substitution of **1** or **2** by the perfluorobutyl group in water: AH stands for the amines **1** or **2**. AC_4F_9 being the substituted amines.

N,N-dialkylamine, one cannot rule out a side-reaction pathway like this to account for the large excess of substrate that we need in our substitution reactions; albeit no *N*-methylaniline **7** was encountered from our irradiations of substrate *N,N*-dimethylaniline **1** in water under our reaction conditions.

It is also known that cyclic voltammetry experiments of **2** in water reveal the presence of dimers



arising from *N,N*-dimethylamino-4-naphthyl radical couplings [32]. No such dimeric products were encountered under our reaction conditions.

Hoffmann and co-workers [17] recently illustrated the photoinduced (350 nm) electron-transfer addition of *N,N*-dimethyl-naphthylamines to electron deficient alkenes in MeCN-H₂O, and postulated the generation of a PET intermediate (the radical cation of the amine) for the rationalization of the products obtained photochemically, supported by a deuterium isotope study [17].

When we subject *N*-methyl-aniline **7** or *N*-methyl-naphthylamine **8** (2-5 equivalents) to a photoreaction (medium pressure Hg lamp, 365 nm) with *n*-C₄F₉I (1 equivalent) in water under vigorous stirring, we obtain the R_F-substitution products in lower yields (32 and 25% yields, respectively, based on *n*-C₄F₉I), albeit the global mass balance for substrate is deficient (> 50%). On the other hand, when we subject primary aromatic amines such as aniline and 1-naphthylamine to the

photoreaction with $n\text{-C}_4\text{F}_9\text{I}$ in water, no appreciable yields of substitution products are encountered.

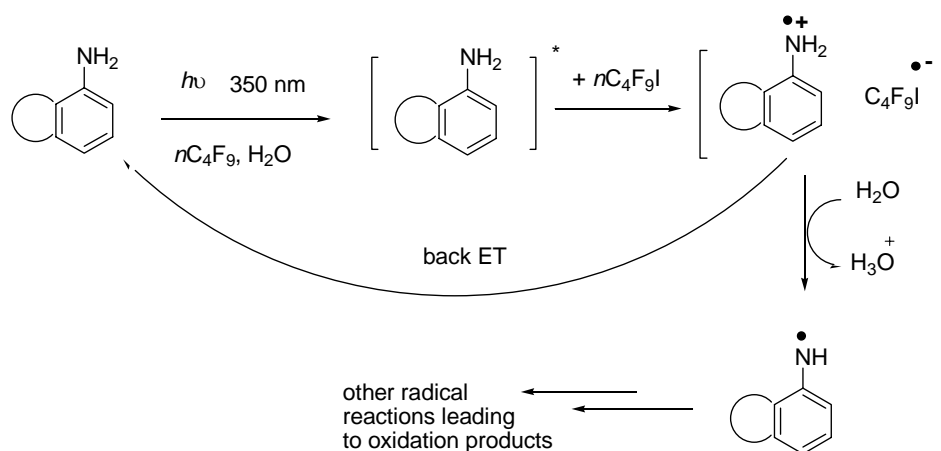
Brede and collaborators have identified two types of radical cations species in the case of secondary aromatic amines, such as **7**, *i.e.*: the planar and perpendicular states. It is obvious that in the planar state (0°) the electron distribution happens over the whole molecule, whereas in the other extreme (90°), the HOMO electrons are fully localized at the nitrogen atom [30]. So, in the cases of secondary aromatic amines, the authors state that the described extremely rapid electron jump can identify all states of bending motion around the -NH- group, resulting in two types of radical cations. The stable amine radical cation is that with delocalized spin distribution, whereas that with the spin localized at the nitrogen atom decays immediately by *deprotonation* (pK_a of *N*-methylaniline radical cation = 7.6 [23a]). Therefore, as we postulate that the PET from **1**, or **2** to $n\text{-C}_4\text{F}_9\text{I}$ arises from population of the n,π^* singlet excited state of the amines (localization of spin distribution on N atom), these dimethyl-substituted and monomethyl-substituted aromatic amines, channel their reactivity into substitution reactions. Probably, the low mass balance obtained from *N*-methylaniline **7**, could be attributed to a deprotonation process of the radical cation $7^{+\bullet}$ as predicted by the studies of Brede and collaborators. In the case of amine **7**, this process is favored from kinetic (oscillation of the N-H bond, in the case of *N*-methylaniline) and energetic reasons,

because the ground level of both states (plane and perpendicular) differs by about 37 kcal mol^{-1} . Then, when the proton affinity of the solvent becomes comparable to or larger than that of the amine radical, this could assist in the deprotonation of the secondary amine radical cation (*i.e.*: *vide infra* Scheme 7 for a primary aromatic amine), depleting substrate concentration. It is likely that deprotonation of *primary* amine radical cations (*i.e.*: pK_a of aniline radical cation = 6.4 [23b,c]) might be much more accelerated in water than deprotonation of *secondary* amine radical cations, diverting the aromatic-ring substitution pathways in the former.

The findings of previous authors reveal that primary and secondary amine radical cations such as those postulated in this work lead to aminyl radicals, whereas tertiary amine radical cations could cause the rapid loss of an $\alpha\text{-H}^+$ to yield α -aminoalkyl radicals or else channel their reactivity otherwise as we observe in this work [33].

Based on the empirical and theoretical ET studies by Brede and collaborators [30], we could interpret the absence of substitution product yields from primary aromatic amines such as aniline or the low substitution yields from secondary aromatic amines, as in Scheme 7 below.

Upon excitation, ArNH_2^* transfers an electron to $n\text{-C}_4\text{F}_9\text{I}$ to render the *in-cage* ET couple $[\text{ArNH}_2^{+\bullet} \ n\text{-C}_4\text{F}_9\text{I}^{\bullet-}]$. Cage-scape of $\text{ArNH}_2^{+\bullet}$ could trigger a series of reactions leading to proton loss and aminyl radical formation, which the latter



Scheme 7. Proposed mechanism for the photoinduced ET oxidation of primary aromatic amines in water.

promptly suffers other radical reactions, ensuing oxidation products (Scheme 7).

Also, Tobita and collaborators have observed that for *N*-methyl-1-naphthylamine [22], the values of τ (singlet excited lifetime) and $\phi_{\text{fluorescence}}$ (Table 3, entries 7 and 8), are lower than those for **2**. The authors attributed the observation to the involvement of a fast non-radiative process in water. The water induced non-radiative processes are remarkable, especially in the compounds with N-H group(s), suggesting that hydrogen-bonding interactions between N-H moiety and water molecule(s) in the excited state are related to the deactivation processes. These deactivating pathways of the excited states of **7** (or **8**), contribute to their lower observed reactivity in the substitution reaction, diverting the excitation towards external conversion processes (hydrogen-bonding), as opposed to *in-cage* ET.

3.3. Aromatic substitution reactions of methoxy-substituted benzenes with R_fX in water

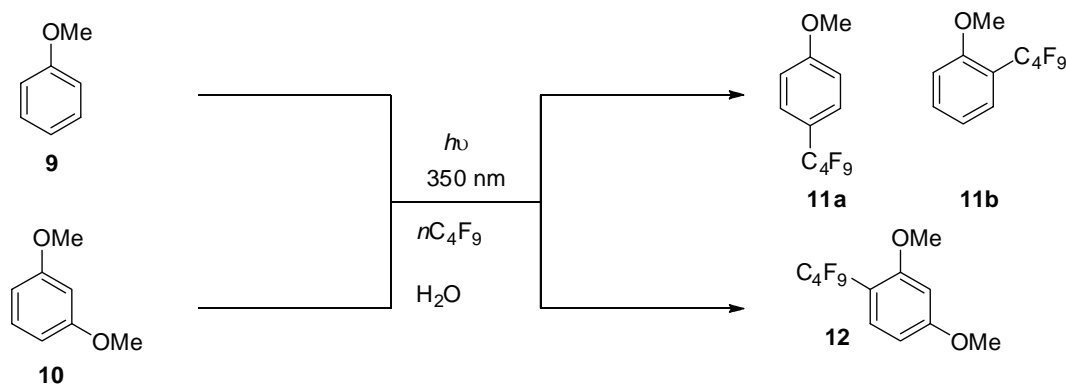
We also subjected methoxy-substituted aromatic compounds, such as anisol **9**, and 1,3-dimethoxybenzene **10**, in water, to the PET reaction with *n*-C₄F₉I, and obtained the aromatic substitution products **11a,b** and **12** in yields 85% and > 80%, respectively, according to Scheme 8 below. The **11a:11b** isomer ratio obtained is 60:40.

The electron-rich methoxy-substituted aromatic substrates **9** and **10** also act as good electron donors to the *n*-C₄F₉I under photostimulation, as is the case for substrates **1**, **2**, and **7**. We surmise

that given the oxidation potential of **10** ($E_{(D/D^+)} = 1.49$ V [33d]), and its excited state (singlet) energy ($E^* = 86$ Kcal/mol) [12], the ΔG_{ET} (**10**→**R_f**) equals -1.2 eV (or -25 Kcal/mol, eq 1), an exergonic process. Unlike the charge transfer quenching of naphthols or phenols that can occur either by electron or proton transfer [34, 35], compounds **9** and **10** could only form a charge transfer complex by electron transfer to **R_f**I. However, the UV-*vis* spectrum of **10** upon addition of *n*-C₄F₉I does not present an additional absorption maximum, neither an exciplex is formed.

It has to be pointed out, that PET from 2-naphthoxide ions to aliphatic halides proceeds with substitution on positions *-1*, *-3*, and *-6* of the naphthalene ring through a radical anion mechanism [36a].

Regarding substrate **9**, previously reported radical substitutions triggered by photodecomposition (185 nm) of azo compounds in benzene as solvent led to a different isomer distribution, *i.e.*: *ortho*-, 40%, *meta*-, 23%, *para*- 37% [36b]. Minisci and co-workers [14] have demonstrated that in the radical perfluorobutylation reaction of various aromatic nuclei (including anisole) in THF as solvent under various radical initiation methodologies, the electrophilic character of *n*-C₄F₉• radical is however scarcely reflected on the orientation of the substitution, *i.e.*: the *ortho*, *meta*, and *para* positions of aromatics are substituted with low selectivity [14]. Our methodology in water leads to substitution at the 4- and 2-positions of the anisole ring, rendering a more regioselective



Scheme 8. Perfluorobutyl group substitution of aromatic methoxy-substituted compounds in water.

radical substitution procedure than the previously reported. It would appear that the orientation is related more to the stabilization of the substituted cation intermediate (electron availability of the ring) rather than the stability of the intermediate radical adducts, which are less sensitive to the substituent position.

In previous studies, the fluorescence emission as well as the triplet-triplet (T-T) absorption of 1-methoxynaphthalene has been studied in the presence of increasing amounts of acceptor 2-(*p*-cyanophenyl)-4-methyl-3-phenyloxetane, to establish the nature of the excited state involved in the PET process [37]. Both singlet and triplet quenching were observed; however, product studies in the presence of triplet quenchers provided evidence that the reaction takes place from the singlet state [38]. The methoxy-substituted aromatic substrates are likely to react from their singlet excited state manifold, ensuing the electron transfer to form radical ion pairs in water.

It has been suggested that in complex systems, with heterogeneous dielectric environments, solute diffusion, structured local environments, and distance-dependent transfer, it is possible to fit the shape and magnitude of data for several donor concentrations [39].

Marcus [26] and others showed that the distance dependence of electron transfer could not be described as a simple exponential representing the falloff of the electronic interaction. It is also necessary to include the distance dependence of the reorganization energy and the free energy change, particularly in heterogeneous systems or microheterogeneous environments. Being radical cation species particularly well-solvated in water, stabilization of this intermediate could lower the rate of back ET, and hence, as in the case of **2**, populate this species ($\mathbf{2}^+$ or **B**) sufficiently enough to act as a ET chain carrier (see Scheme 7, Figure 3).

For donors and acceptors diffusing in a liquid, it is not sufficient to consider electron transfer and geminate recombination as only occurring at contact, nor is it sufficient (possible) to describe the liquid as a homogeneous continuum. We hereby treat a heterogeneous system where proper ensemble averages over the spatial distribution of donors and acceptors are required. The electron

transfer problem becomes even more intricate for systems with complex geometries as evidenced by the recent activity describing electron transfer in DNA [40]. As systems (*e.g.*, DNA) become more complex, there is a natural tendency to simplify the description, leaving out aspects that are known to be important in other contexts.

The work presented herein on a heterogeneous system is an attempt to describe electron-transfer dynamics in a finite volume, in a manner that accounts for the major aspects of the problem. The theory has been earlier presented for micelles [39] and is a description of electron transfer in a heterogeneous environment, including factors that are known to be necessary to describe electron transfer in liquids plus additional components that are necessary to capture the essential nature of the micelle problem. We surmise that in a pronounced heterogeneous system, such as that described here, the interpretation of ET could result far more complex. We surmise that in our heterogeneous system, the local reagents concentrations (particularly that of *n*-C₄F₉I) at the irradiation wavelength, is much lower than the expected in MeCN, allowing the ET from substrates to R_fI, and precluding direct homolysis of *n*-C₄F₉I. The very heterogeneity of our medium diverts the simple homolytic substitution mechanism to a radical ion chain reaction.

The experiments and theory point the way to a deeper understanding of electron transfer in complex environments. Further experiments are in progress in order to study the PET perfluoroalkylation of electron-rich aromatic compounds in other heterogeneous and microheterogeneous media.

CONCLUSIONS

We have shown that aromatic amines such as *N,N*-dimethylaniline, *N,N*-dimethyl-1-naphthyl amine, and methoxy-substituted aromatics react in water by PET with R_fX to render substitution products in fairly good yields. Of note is the fact that the proposed mechanism involves a radical ion chain process, accounting for the observed yields of substitution products, where the radical cations of the substrates are formed in the initiation event, and a radical chain mechanism seems superimposed with a redox chain. Concerning some

mechanistic details, the reaction is compared with radical and electrophilic aromatic substitutions. Taking into account the local absorbances at the irradiation wavelength, we could speculate that our heterogeneous reaction media precludes even more the direct homolysis of the F₉C₄-I bond, and restricts direct homolytic substitution of the ring.

ACKNOWLEDGMENT

Thanks are given to financial agencies such as Conicet-Argentina, and Agencia Nacional de Promoción Científica y Técnica, Argentina, PICTO-CRUP 30891 is gratefully acknowledged. We acknowledge Prof. Dra. Alicia B. Peñéñory and Prof. Dr. Juan E. Argüello for running the NLFP experiments. Thanks are also given to Sebastián Barata-Vallejo, Marina Martin Flesia and Beatriz Lantaño for the results on aromatic amines.

REFERENCES

1. Barata-Vallejo, S. and Postigo, A. 2010, *J. Org. Chem.*, 75, 6141-6148.
2. (a) Slodowicz, M., Barata-Vallejo, S., Vázquez, A., Nudelman, N. and Postigo, A. 2012, *J. Fluor. Chem.*, 135, 137-143. (b) Postigo, A. 2012, *Can. J. Chem.*, 90, 493-497.
3. Barata-Vallejo, S. and Postigo, A. 2012, *Eur. J. Org. Chem.*, 2012, 1889-1899.
4. Dmowski, W., Urbanczyk-Lipkowska, Z. and Wójcik, D. 2009, *J. Fluor. Chem.*, 130, 509-511.
5. Dmowski, W. and Piasecka-Maciejewska, K. 2010, *J. Fluor. Chem.*, 131, 746-750.
6. (a) Qi, Q., Shen, Q. and Lu, L. 2012, *J. Fluor. Chem.*, 133, 115-119. (b) Qi, Q., Shen, Q. and Lü, L., 2011, *Chin. J. Chem.*, 29, 2681-2683.
7. Huang, W. and Ma, W. 1992, *Chin. J. Chem.*, 10, 180-185.
8. Cao, H. P., Xiao, J-C. and Chen, Q-Y. 2006, *J. Fluor. Chem.*, 127, 1079-1082.
9. Loy, R. N. and Sanford, M. S. 2011, *Org. Lett.*, 13, 2548-2551.
10. (a) Ohtsuka, Y. and Yamakawa, T. 2011, *Tetrahedron*, 67, 2323-2331. (b) Kino, T., Nagase, Y., Ohtsuka, Y., Yamamoto, K., Uruguchi, D., Tokuhisa, K. and Yamakawa, T. 2010, *J. Fluor. Chem.*, 131, 98-105.
- (c) Murakami, S., Ishii, H., Tajima, T. and Fuchigami, T. 2006, *Tetrahedron*, 62(15), 3761-3769.
11. (a) Cuquerella, M. C., Boscá, F. and Miranda, M. A. 2004, *J. Org. Chem.*, 69, 7256-7261. (b) Barata-Vallejo, S., Martín Flesia, M., Lantaño, B., Argüello, J. E., Peñéñory, A. B., Postigo, A. 2013, *Eur. J. Org. Chem.*, 998-1008. (c) Kiyota, T., Yamaji, M. and Shizuka, A. 1996, *J. Phys. Chem.*, 100, 672-679. (d) Yamaji, M., Kiyota, T. and Shizuka, H. 1994, *Chem. Phys. Lett.*, 226, 199-205.
12. Rong, X. X., Pan, H.-Q. and Dolbier, W. R. Jr. 1994, *J. Am. Chem. Soc.*, 116, 4521-4522.
13. (a) Davis, C. R., Burton, D. J. and Yang, Z.-Yu. 1995, *J. Fluor. Chem.*, 70, 135-140. (b) Le, T. D., Arlauskas, R. A. and Weers, J. G. 1996, *J. Fluor. Chem.*, 78, 155-163. (c) Huang, X.-T. and Chen, Q.-Y. 2001, *J. Org. Chem.*, 66, 4651-4656. (d) Scannell, M. P. Fenick, D. J., Syun-Ru Yeh and Falvery, D. E. 1997, *J. Am. Soc.*, 119, 1971-1977.
14. Bravo, A., Bjørsvik, H-R., Fontana, F., Liguori, L., Mele, M. and Minisci, F. 1997, *J. Org. Chem.*, 62, 7128-7136.
15. Calandra, J., Postigo, A., Russo, D., Sbarbati Nudelman, N. and Tereñas, J. J. 2010, *J. Phys. Org. Chem.*, 23, 944-949.
16. Darmanyan, A. P. and Jenks, W. S. 1998, *J. Phys. Chem. A*, 102, 7420-7426.
17. (a) Jahjah, R., Gassama, A., Dumur, F., Marinkovic, S., Richert, S., Landgraf, S., Lebrun, A., Cadiou, C., Sellesz, P. and Hoffmann, N. 2011, *J. Org. Chem.*, 76, 7104-7118. (b) Griesbeck, A. G., Hoffmann, N. and Warcecha, K. D. 2007, *Acc. Chem. Res.*, 40, 128-140.
18. Nova, A. I., Borsarelli, C. D., Cosa, J. J. and Previtali, C. M. 1998, *J. Photochem. Photobiol. A Chemistry*, 115, 43-47.
19. Andrieux, C. P., GClis, L., Medebielle, M., Pinson, P. and Saveant, J. M. 1990, *J. Am. Chem. Soc.*, 112, 3509-3520.
20. Zweig, A., Hodgson, W. G. and Jura, W. H. 1964, *J. Am. Chem. Soc.*, 86, 4124-4129.
21. Berman, I. B. 1971, *Handbook of Fluorescence Spectra of Aromatic Molecules*, Academic: New York.

-
22. Tobita, S., Ida, K. and Shiobara, S. 2001, *Res. Chem. Intermed.*, 27, 205-218.
 23. (a) Jonsson, M., Wayner, D. D. M. and Luszyk, J. 1996, *J. Phys. Chem.*, 100, 17539-17543. (b) Yu, A., Liu, Y., Li, Z. and Cheng, J-P. 2007, *J. Phys. Chem. A*, 111, 9978-9987. (c) Bordwell, F. G., Zhang, X-M. and Cheng, J-P. 1993, *J. Org. Chem.*, 58, 6410-6416.
 24. Lampert, R. A., Chewter, L. A. and Phillips, D. 1983, *Anal. Chem.*, 55, 68-73.
 25. Ebersson, L. 1987, *Electron Transfer Reactions in Organic Chemistry*, Springer-Verlag; Berlin, Germany.
 26. (a) Sutin, N. 1991, Nuclear and Electronic Factors in Electron Transfer: Distance Dependence of Electron-Transfer Rates. In *Electron Transfer in Inorganic, Organic, and Biological Systems*; Bolton, J. R., Mataga, N., McLendon, G. (Eds.), The American Chemical Society, Washington, p 25. (b) Marcus, R. A. 1956, *J. Chem. Phys.*, 24, 966. (c) Marcus, R. A. 1956, *J. Chem. Phys.*, 24, 979. (d) Marcus, R. A. 1964, *Annu. Rev. Phys. Chem.*, 15, 155. (e) Marcus, R. A. and Sutin, N. 1985, *Biochim. Biophys. Acta*, 811, 265. (f) Bolton, J. R. and Archer, M. D. 1991, Basic Electron-Transfer Theory. In *Electron Transfer in Inorganic, Organic, and Biological Systems*; Bolton, J. R., Mataga, N. and McLendon, G. (Eds.), The American Chemical Society, Washington, p 7.
 27. Inada, T. N., Kikuchi, K., Takahashi, Y., Ikeda, H. and Miyashi, T. 2000, *J. Photochem. Photobiol. A: Chem.*, 137, 93-97.
 28. Kikuchi, K., Hoshi, M., Niwa, T., Takahashi, Y. and Miyashi, T. 1991, *J. Phys. Chem.*, 95, 38-42.
 29. Holcman, J. and Sehested, K. 1977, *J. Phys. Chem.*, 81, 20-26.
 30. Maroz, A., Hermann, R., Naumov, S. and Brede, O. 2005, *J. Phys. Chem. A*, 109, 4690-4696.
 31. Baciocchi, E., Bietti, M., Gerini, M. F. and Lanzalunga, O. 2005, *J. Org. Chem.*, 70, 5144-5149.
 32. Vettorazzi, N., Fernandez, H., Silber, J. J. and Sereno, L. 1990, *Electrochem. Acta*, 35, 1081-1088.
 33. (a) Karakostas, N., Naumov, S. and Brede, O. 2009, *J. Phys. Chem. A*, 113, 14087-14094. (b) Zeng, C-C. and Becker, J. Y. 2004, *J. Org. Chem.*, 69, 1053-1069. (c) Fukuzumi, S., Yuasa, J., Satoh, N. and Suenobu, T. 2004, *J. Am. Chem. Soc.*, 126, 7585-7594. (d) Dileesh, S. and Gopidas, K. R. 2000, *Chem. Phys. Lett.*, 330, 397-402.
 34. Tolbert, L. M. and Nesselroth, S. M. 1991, *J. Phys. Chem.*, 95, 10331-10336.
 35. Leheny, A. R., Turro, N. J. and Drake, J. M. 1992, *J. Phys. Chem.*, 96, 8498-8502.
 36. (a) Arguello, J. E. and Peñéñory, A. B. 2003, *J. Org. Chem.*, 68, 2362-2368. (b) Nakamura, T. and Koga, Y. 1998, *J. Chem. Soc., Perkin Trans.*, 2, 659-662.
 37. Pérez-Ruiz, R., Izquierdo, M. A. and Miranda, M. A. 2003, *J. Org. Chem.*, 68, 10103-10108.
 38. Pérez-Ruiz, R., Gil, S. and Miranda, M. A. 2005, *J. Org. Chem.*, 70, 1376-1381.
 39. Tavernier, H. L., Laine, F. and Fayer, M. D. 2001, *J. Phys. Chem. A*, 105, 8944-8957.
 40. Lewis, F. D., Kalgutkar, R. S., Wu, Y. S., Liu, X. Y., Liu, J. Q., Hayes, R. T., Miller, S. E. and Wasielewski, M. R. 2000, *J. Am. Chem. Soc.*, 122, 12346-12351.